

Dependence of the Electrical Conductivity and Thermoelectric Power of Pure and Aluminum-Doped Rutile on Equilibrium Oxygen Pressure and Temperature*

J. YAHIA†

National Bureau of Standards, Washington, D. C.

(Received 12 September 1962; revised manuscript received 31 January 1963)

The electrical conductivity σ and thermoelectric power Q have been measured as a function of equilibrium oxygen pressure in crystals of pure and Al-doped rutile. The pressure was varied over the range 10^{-4} mm Hg to $\sim 10^8$ mm Hg with the temperature held constant at several fixed values in the vicinity of 1000°K. The electrical conductivity of the pure material varied with pressure according to the relation $\sigma \propto p^{-1/x}$ with $x \approx 6$ for $p > 10$ mm Hg and $x \approx 5$ for $p < 10$ mm Hg. For the Al-doped crystal, σ reached a minimum for $p = p_0$ mm Hg. At low pressures σ followed a relation of the form $\sigma \propto p^{-1/x}$ with $x \sim 5$, whereas at high pressures a relation of the form $\sigma \propto p^{+1/x}$ with $x \sim 5$ was obeyed. The thermoelectric power exhibited a reversal near p_0 , being negative at lower pressures and positive for $p > p_0$. For pure rutile a defect model involving anion vacancies and estimated values of equilibrium constants leads to a pressure dependence of the conductivity: $\sigma \propto p^{-1/6}$, whereas for a model involving titanium interstitials the pressure dependence is $\sigma \propto p^{-1/5}$. On the basis of the present measurements it seems that for pure rutile the anion vacancy mechanism obtains at "high" pressures with the titanium interstitials mechanism predominating at "low" pressures. For Al-doped rutile, both the anion vacancy model and the titanium interstitials model are shown to give rise to approximately the observed pressure dependence of conductivity. The anion vacancy model equations are solved in detail (assuming certain values of the equilibrium constants). The titanium interstitials model equations are not solved explicitly for this case but it is shown that for a certain combination of reaction constants the observed pressure dependence may be approximated. Assuming a two-band formalism to be valid—and therefore, a formalism into which the results derived from any defect model must fit—we have analyzed the data and shown that reasonable agreement with observation results. Some indications that hole mobilities at 1000°K are considerably larger (~ 180 cm²/V sec) than those of the electrons are discussed. Assuming high-temperature polar scattering to obtain, a hole effective mass $10^{-2} m_0$ (where m_0 is the free-electron mass) is deduced as a consequence of the mobility calculations.

I. INTRODUCTION

THE extrinsic electronic properties of oxide semiconductors depend on lattice defects such as (a) deviations from stoichiometry due to the interaction of the pure substance with the surrounding atmosphere or (b) foreign ions in the lattice. These defects can form donors or acceptors with resulting n - and p -type conductivity, respectively. Examples of (a) are afforded by TiO₂, ZnO, BaTiO₃, and Cu₂O, NiO. TiO₂ and ZnO are known as "reduction" semiconductors since they lose oxygen readily to become n -type conductors. On the other hand, Cu₂O and NiO are known as "oxidation" semiconductors since the metal ion tends to take on a higher valency with the taking up of excess oxygen. For a "reduction" semiconductor with no chemical impurities, the conductivity usually decreases with increasing oxygen pressure, whereas for an "oxidation" semiconductor, the conductivity usually increases with increasing oxygen pressure.^{1,2} An example of (b) is NiO containing Li⁺ ions.³ In this case, the presence of the Li⁺ induces the formation of a Ni³⁺ in the Ni²⁺ lattice so that p -type conduction is produced in this "mixed valency" substance. Kroger, Vink, and van den

Boomgaard⁴ give a discussion of controlled conductivity in cadmium sulfide where the influence of defects on the conductivity is considered in detail.

The electronic properties of rutile have been extensively investigated.⁵ As a result of this work, the properties of electrons in rutile are rather well known. The electron is generally believed to travel in a narrow $3d$ band with effective mass $\sim 30m_0$ (where m_0 is the free-electron mass); the mobility is governed by polar scattering at high temperatures and by scattering by impurities at intermediate temperatures.⁶ A survey of recent studies on rutile is given by Frederikse⁷ and by von Hippel *et al.*⁸ In contrast to the situation for n -type TiO₂, information concerning p -type rutile is quite limited. The first detailed study of holes in rutile was that of Rudolph² who observed a positive thermoelectric power in his iron-doped sintered samples. The author has confirmed Rudolph's results on single-crystal material and briefly reported p -type behavior in Al-doped material.⁹ The object of the present investigation was twofold: first, to obtain information concerning the nature of the defect centers contributing to the

⁴ F. J. Kröger, H. J. Vink, and van den Boomgaard, *Z. Physik. Chem.* **203**, 1 (1954).

⁵ Cf. appropriate sections of F. A. Grant's excellent review article on rutile in *Rev. Mod. Phys.* **31**, 646 (1959).

⁶ R. G. Breckenridge and W. R. Hosler, *Phys. Rev.* **91**, 793 (1953).

⁷ H. P. R. Frederikse, *Suppl. J. Appl. Phys.* **32**, 2211 (1961).

⁸ A. von Hippel, J. Kalnajs, and W. B. Westphal, *J. Phys. Chem. Solids* **23**, 779 (1962).

⁹ J. Yahia, *Bull. Am. Phys. Soc.* **1**, 221 (1962).

* Research supported in part by the Office of Naval Research.

† Present address: Pennsylvania State University, Physics Department, University Park, Pennsylvania.

¹ K. Hauffe, *Reaktionen in und an Festen Stoffen* (Springer-Verlag, Berlin, 1955).

² J. Rudolph, *Z. Naturforsch.* **14a**, 727 (1959).

³ E. J. W. Verwey, P. W. Haaijman, and F. C. Romeijn, *Chem. Weekblad* **44**, 705 (1948).

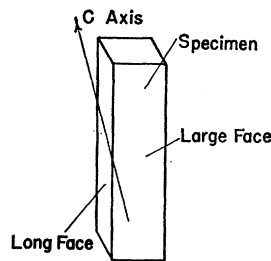


FIG. 1. Identification of faces in samples.

production of electrons and holes, which is a question of considerable interest;¹⁰⁻¹³ second, to gain knowledge of the motion of holes in rutile. Both pure and Al-doped crystals have been investigated. Aluminum was selected as the doping agent, since, like Fe, it would be expected to give rise to *p*-type conductivity, but unlike Fe, the Al ion is believed to exist in only one valence state, a factor simplifying the analysis.

II. EXPERIMENTAL CONSIDERATIONS

A. Samples and Electrical Connections

The samples were cut from single-crystal boules grown by the Verneuil flame fusion technique. A controlled amount of Al was introduced into the rutile lattice by mixing into the starting rutile powder the appropriate amount of aluminum oxide. The dominant impurities in the starting TiO₂ powder were: SiO₂ (0.05 wt. %), Fe₂O₃ (0.001), Al₂O₃ (<0.001), Sb₂O₃ (<0.001), SnO₂ (<0.001), Mg (0.0005), Nb (<0.01), Cu (0.0003), Pb (<0.001), Mn (<0.00005), W (<0.005), V (<0.001), Cr (<0.001). These were determined by spectrographic analysis. A powder x-ray picture taken of part of the Al-doped boule showed that the rutile structure was preserved.¹⁴ No attempt at orienting the crystals was made, since the emphasis in this study was not in that direction; however, the orientation of the single crystals is included for completeness. For the Al-doped crystal, the *c* axis makes an angle of 16° with the large face and 10° with the long edge plane. For the pure crystal, the *c* axis makes an angle of 19° with the large face and 15° with the long edge plane.¹⁵ The crystal faces are defined in Fig. 1. The electrical contacts to the crystal were made by force fitting electrodes into tiny holes (0.015-in. diam) drilled into the crystal

¹⁰ Cf., E. H. Greener, D. H. Whitmore, and M. E. Fine, *J. Chem. Phys.* **34**, 1017 (1961). Equation (10) of this article should be a cubic rather than a quadratic; Eq. (11b) should read $[\theta] \ll 2K_3$.

¹¹ T. Hurlen, *Acta Chem. Scand.* **13**, 365 (1959).

¹² W. R. Buessem and S. R. Butler, in *Kinetics of High Temperature Processes*, edited by E. Kingery (John Wiley & Sons, Inc., New York, Tech. Press, Cambridge, Massachusetts, 1958).

¹³ T. Koifstad, *J. Phys. Chem. Solids* **23**, 1579 (1962).

¹⁴ The author wishes to thank M. Cohen of the Solid State Physics Section, National Bureau of Standards, and J. Swanson of the Constitution and Microstructure Section, National Bureau of Standards, for this result.

¹⁵ Thanks are due M. Cohen of the Solid State Physics Section for these results obtained from Laue x-ray photographs.

by means of a "cavitron." The position of the leads and typical dimensions for the crystals are shown in Fig. 2.

B. Controlled Oxygen Pressure System and Ovens

The sample was placed horizontally in a quartz tube (o.d. 1/2 in.) which formed part of a system for maintaining a controlled pressure of oxygen gas around the sample. At high pressures, a certain amount of gas was introduced into the quartz tube from a reservoir and the system allowed to come to static equilibrium. For the low pressures, a dynamic equilibrium was preferred whereby gas was introduced into the combustion tube at one end and pumped out at the other end. For high pressures the measuring instruments used were a mercury manometer and a Dubrovin gauge. For the low pressures McLeod gauges were used. All of these instruments were trapped by using traps filled with solid CO₂+ethyl alcohol mixture to prevent mercury from entering the experimental chamber. There were two ovens in this equipment. A small (diameter slightly larger than that of the quartz tube) platinum-wound lava or quartz core oven was placed at the proper position with respect to the sample within the tube to give as large a temperature gradient as was desired (usually ~20-30°K). This temperature gradient was reversed for some of the measurements by moving the Pt heater along the quartz tube. The observations were independent of direction of the temperature gradient. Around this oven a much larger oven was placed, mainly to stabilize temperatures. With this system, temperature gradients ~30°K were easily obtained at 1000°K, remaining constant over long periods of time. Controlled currents were supplied to the oven by means of variacs, or adjustable resistors were used when operating on dc.

C. Electrical Measurements

Electrical measurements were made using a Leeds and Northrup Type K-3 potentiometer. Temperatures were obtained using (Pt-PtRh) thermocouples I and II (see Fig. 2). Using the platinum arms of the thermocouples, the Seebeck voltage was determined. Measurements of temperature and Seebeck voltage give the thermoelectric power. Conductivity was measured by passing a current through the crystal and observing the voltage between the platinum arms of the thermocouples for the current first in one direction, then in the opposite direction. Care had to be taken to keep impressed fields

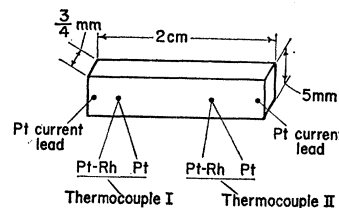


FIG. 2. Electrical leads to crystals and typical dimensions of crystals.

to a small size, otherwise polarization difficulties would arise.¹⁶ It was advantageous to shield electrically the crystal from extraneous fields by wrapping platinum foil around the quartz tube.

D. Experimental Results

The experimental observations are shown in Figs. 3 and 4. The variation of the electrical conductivity with pressure at a few fixed temperature points is shown in Fig. 3 for pure rutile. The pressure dependence is given by the following relation: $\sigma \propto p^{-1/x}$ with $x \cong 5$ for $p < 10$ mm Hg and $x \cong 6$ for $p > 10$ mm Hg. The thermoelectric power and electrical conductivity as functions of the pressure at a few fixed temperatures for Al-doped rutile are shown in Fig. 4. The outstanding features shown here are: (1) the occurrence of a minimum in the conductivity at a pressure p_0 ; (2) At high temperatures, for pressures greater than p_0 the conductivity varies as $p^{+1/x}$ while for pressures smaller than p_0 , $\sigma \propto p^{-1/x}$ where p is the equilibrium oxygen pressure and x is about 5; (3) A reversal in the sign of Q , the thermoelectric power, occurs near p_0 . At high pressures Q is positive while it is negative at low pressures. (4) The minimum in conductivity shifts to higher pressures as the temperature is increased. Furthermore, the pressure at which $Q=0$

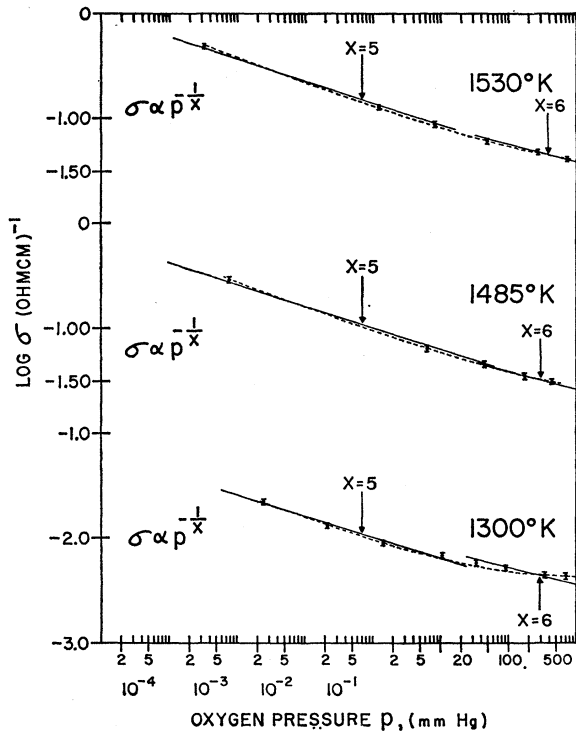


FIG. 3. Oxygen pressure dependence of electrical conductivity for pure rutile.

¹⁶ Rebecca A. Parker and J. H. Wasilik [Phys. Rev. 120, 1631 (1960)], have also observed this effect.

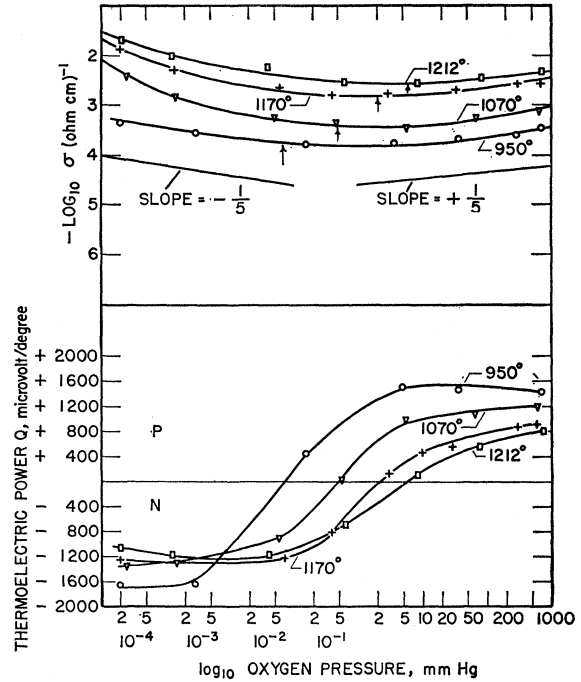


FIG. 4. Oxygen pressure dependence of electrical conductivity (top) and thermoelectric power (bottom) for aluminum-doped rutile. Crystal II, Al-doped 0.5%.

shifts with temperature somewhat like that for the conductivity minimum.

III. ANALYSIS OF ELECTRICAL CONDUCTIVITY RESULTING FROM VARIOUS MODELS FOR THE DEFECTS

We will calculate the dependence on pressure of the concentrations of electrons and holes using two models for the defects in both pure and aluminum-doped rutile. The assumption will be made that at high temperatures the mobility is independent of the concentration of defects. In this way, a comparison of the experimental conductivity data and that obtained from calculation will be used to test which model is the more applicable.

Case 1. Pure Nonstoichiometric Rutile

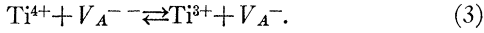
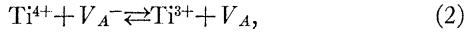
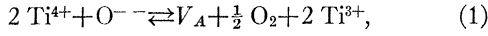
(a) Anion Defects Model

For this case, the following defects will be assumed to be present in the crystal:

- (i) Ti^{3+} at a normal lattice position: (a quasifree electron in the Ti 3d band),
- (ii) V_A : (an anion vacancy),
- (iii) V_A^- : (an anion vacancy with one trapped electron),
- (iv) V_A^{--} : (an anion vacancy with two trapped electrons).

The above assignment of defects considers an ionic model and the reaction of the crystal with its surround-

ing atmosphere to give rise to anion vacancies and Ti^{3+} in normal lattice positions. The reactions between the defects may be written as follows:



Since our data for undoped rutile indicated extrinsic n -type conduction, the intrinsic reaction $\text{Ti}^{4+} + \text{O}^{-} \rightleftharpoons \text{Ti}^{3+} + \text{O}^{-}$ and other hole-producing reactions will not be included in the calculations.

Equation (1) represents the production of anion vacancies and the formation of Ti^{3+} on lattice sites as well as the loss of oxygen from the crystal to the surrounding atmosphere; Eq. (2) represents the ionization of a V_A^{-} forming a V_A and a Ti^{3+} ; Eq. (3) represents the ionization of a V_A^{-} forming a V_A^{-} and a Ti^{3+} .

The law of mass action applied to the reactions (1) to (3) leads to the equations:

$$[V_A][\text{O}_2]^{1/2}[\text{Ti}^{3+}]^2 = K_2(T), \quad (4)$$

$$[\text{Ti}^{3+}][V_A]/[V_A^{-}] = K_3(T), \quad (5)$$

$$[\text{Ti}^{3+}][V_A^{-}]/[V_A^{-}] = K_4(T). \quad (6)$$

The K 's are reaction constants which may be evaluated under special assumptions. In addition to Eqs. (4)–(6), the electroneutrality condition gives the following equation:

$$[\text{Ti}^{3+}] = [V_A^{-}] + 2[V_A]. \quad (7)$$

In all of these equations, the square brackets indicate concentration of the defect involved.

If Eq. (4) is rewritten for convenience as

$$[V_A][\text{Ti}^{3+}]^2 = K_2(T)[\text{O}_2]^{-1/2} = K_2'(T),$$

the solution of the set (4) to (7) may be obtained as:

$$[V_A] = (K_3^2/K_2') [V_A^{-}]^2, \quad (8)$$

$$[\text{Ti}^{3+}] = (K_2'/K_3) [V_A^{-}]^{-1}, \quad (9)$$

$$[V_A^{-}] = K_2'/K_3 K_4, \quad (10)$$

$$[V_A^{-}]^3 + (K_2'/2K_3^2) [V_A^{-}]^2 - K_2'^2/2K_3^3 = 0. \quad (11)$$

Equations (8)–(10) give $[V_A]$, $[\text{Ti}^{3+}]$, $[V_A^{-}]$ as functions of $[V_A^{-}]$ and the reaction constants K_2' , K_3 , and K_4 . Equation (11) is an equation for $[V_A^{-}]$ in terms of the reaction constants K_2' , K_3 . Equation (11) may be readily solved if the values of K_2' and K_3 are known. A value of K_2' may be taken from the work of Buessem and Butler¹² who calculate an experimental value of K_2' from weight loss measurements. K_2' is given (at 1170°K) as $2.4 \times 10^{61} p^{-1/2}$ where p is the pressure in mm Hg. The value of K_3 may be estimated as follows. A V_A^{-} may be represented roughly as a singly ionized

TABLE I. Calculated values of $[V_A^{-}]$ and $[\text{Ti}^{3+}]$ as functions of oxygen pressure at 1170°K in pure rutile. Oxygen vacancy model assuming various parameters discussed in the text.

O ₂ pressure (mm Hg)	10 ⁻⁴	10 ⁻²	1	10 ³
$[V_A^{-}]$ (per cc)	1.7×10^{21}	3.8×10^{20}	8.3×10^{19}	8.3×10^{18}
$[\text{Ti}^{3+}]$ (per cc)	1.8×10^{21}	7.9×10^{20}	3.6×10^{20}	1.2×10^{20}

helium atom.¹⁷ The energy required to ionize the V_A^{-} is accordingly given by¹⁸

$$\epsilon_{2\text{-ion}}(\text{eV}) = (m^*/m_0)K^{-2} \times (54.4),$$

where m^* is the effective mass of the electron, m_0 is the free-electron mass, and K is the static dielectric constant (~ 70 in rutile at 1170°K).¹⁹ m^* is taken to be $\sim 30m_0$, a reasonable value judging from previously published work.^{5,6} With these assumptions $\epsilon_{2\text{-ion}} = 0.3$ eV, K_3 is then given by³

$$K_3(T) = \left(\frac{2\pi(m^*/m_0)kT}{h^2} \right)^{3/2} \exp[-(\epsilon_{2\text{-ion}}/kT)],$$

where T is the absolute temperature, h is Planck's constant, and k is Boltzmann's constant. At $T = 1170^\circ\text{K}$, K_3 has the value $8.10^{20} \text{ cm}^{-3}$. Further, since the first ionization energy of a He-like defect is considerably smaller than the second ionization energy, we conclude $K_4 \gg K_3$. Table I shows how $[V_A^{-}]$ and $[\text{Ti}^{3+}]$ depend on pressure. Figure 5 shows a plot of $\log[\text{Ti}^{3+}]$ vs $\log p$ as obtained from the calculated values of Table I. The straight line has the slope²⁰ $-(1/6)$.

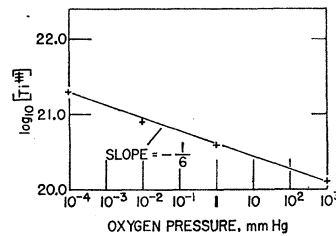


FIG. 5. $\log[\text{Ti}^{3+}]$ vs $\log p$ from the calculated values in Table I.

¹⁷ D. C. Cronemeyer and M. A. Gilleo, Phys. Rev. **82**, 975 (1951).

¹⁸ H. Brooks, in *Advances in Electronics and Electron Physics*, edited by L. Marton (Academic Press Inc., New York, 1955), Vol. VII.

¹⁹ Rebecca A. Parker, Phys. Rev. **124**, 1719 (1961).

²⁰ This result could have been predicted by a consideration of Eq. (11) in the following limiting case. This equation may be written as

$$[V_A^{-}]^3 + (K_2'/2K_3^2) ([V_A^{-}]^2 - K_2'/K_3) = 0.$$

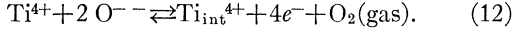
If $K_2'/K_3 \gg [V_A^{-}]^3$, then

$$[V_A^{-}]^3 - K_2'^2/2K_3^3 \cong 0, \quad \text{or} \quad [V_A^{-}] = (1/2K_3^2)K_2'^2/3 = \text{const } p^{-1/3}.$$

Thus, for this case, $[\text{Ti}^{3+}] \propto p^{-1/6}$. A look at Table I will show that this result is plausible, for already at $p = 10^{-2}$ mm, $K_2'/K_3 = 3 \times 10^{41}$, $[V_A^{-}]^2 = 1.4 \times 10^{41}$, and therefore, $K_2'/K_3 > [V_A^{-}]^2$. The physical picture here is one of nearly complete ionization of the V_A^{-} and V_A^{-} with only V_A and Ti^{3+} remaining as defect centers. On the other hand, if V_A^{-} remains a dominant defect, $[\text{Ti}^{3+}] \propto p^{-1/4}$ results. These limiting cases have been calculated by various workers (references 1, 8, 10, 11).

(b) *Titanium Interstitials Model*

The reaction of the crystal with its surrounding oxygen atmosphere may take place according to the following reaction¹¹



$\text{Ti}_{\text{int}}^{4+}$ is a titanium ion at an interstitial position; e^- is a quasifree electron. If we assume that the four electrons are then distributed to four Ti^{4+} on normal lattice sites, then e^- is equivalent to Ti^{3+} . Using the law of mass action, one may write

$$[\text{Ti}_{\text{int}}^{4+}] \cdot [\text{Ti}^{3+}]^4 p = K_1(T), \quad (13)$$

where p is the oxygen pressure and K_1 a reaction constant. Furthermore, the electroneutrality relation becomes

$$[\text{Ti}^{3+}] = 4[\text{Ti}_{\text{int}}^{4+}]. \quad (14)$$

Equations (13) and (14) give the result that $[\text{Ti}^{3+}] \propto p^{-1/5}$. On the basis of the experimental $\log \sigma$ vs $\log p$ curves for pure rutile (Fig. 3) it appears that a $p^{-1/5}$ dependence is followed at pressures < 10 mm Hg, while at pressures above this a $p^{-1/6}$ dependence is obeyed. Therefore, it seems that the anion vacancy mechanism predominates at "high" pressures while the titanium interstitials mechanism is dominant at "low" pressures. The $p^{-1/6}$ dependence is in agreement with the work of Buessem and Butler¹² which involves weight loss measurements and a self-consistent calculation of the reaction constants using the data. Kofstad¹³ also observes a $p^{-1/6}$ dependence in his published results on thermogravimetric measurements in rutile. The $p^{-1/5}$ dependence is more along the line of reasoning presented by Hurlen.¹¹ It must be pointed out, however, that the value of the pressure exponent $1/x$ depends on the range of pressure and temperature over which the measurements are made. Thus, Earle²¹ finds that $1/x$ varies from $-1/2$ to $-1/4.3$ and the measurements of Hauffe²² show a variation of $1/x$ from $-1/4.4$ to $-1/5.3$.

Case 2. Al-Doped Nonstoichiometric Rutile

(a) *Anion Vacancies, Al^{3+}O^- Acceptors*

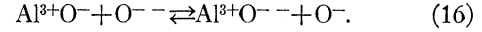
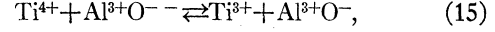
The following defects will be assumed to be present in addition to those considered in Case 1(a) above:

- (i) O^- in a lattice position: a hole in the oxygen $2p$ band,
- (ii) Al^{3+}O^- : a filled Al-O level,
- (iii) Al^{3+}O^- : an unfilled Al-O level.

This assignment of defects considers the aluminum to enter substitutionally into the lattice replacing a Ti^{4+} at normal lattice sites. It is assumed that V_c , V_c^{++} , V_c^{3+} , V_c^{4+} do not exist (V_c is cation vacancy, V_c^+ is a cation vacancy of plus one charge, etc.). In the absence

of V_c , the mechanism of hole formation is shown in Eq. (16) following.

The reactions to be considered are the ones given for Case 1(a) above and the following:



Equation (15) represents the emptying of an Al level forming Al^{3+}O^- and a Ti^{3+} . Equation (16) represents the filling of an Al level forming $\text{Al}^{3+}\text{O}^{--}$ and an O^- in the oxygen $2p$ band. The law of mass action applied to the reactions (15) and (16) leads to the equations

$$[\text{Ti}^{3+}][\text{Al}^{3+}\text{O}^-]/[\text{Al}^{3+}\text{O}^-] = K_5(T), \quad (17)$$

$$[\text{Al}^{3+}\text{O}^{--}][\text{O}^-]/[\text{Al}^{3+}\text{O}^-] = K_6(T). \quad (18)$$

The electroneutrality condition is now written as

$$[\text{Ti}^{3+}] + [\text{O}^- - \text{Al}^{3+}] = [\text{O}^-] + [V_A^-] + 2[V_A]. \quad (19)$$

Finally, the total aluminum concentration in the crystal must equal the sum of the filled and unfilled Al levels,

$$[\text{O}^- - \text{Al}^{3+}] + [\text{O} - \text{Al}^{3+}] = [\text{Al}^{3+}]. \quad (20)$$

The intrinsic reaction producing holes and electrons is included in Eqs. (17) and (18). The solution to Eqs. (4)–(6), (17)–(20) may be written as follows:

$$[\text{Ti}^{3+}] = (K_2'/K_3)(1/[V_A^-]), \quad (21)$$

$$[V_A] = (K_3^2/K_2')[V_A^-]^2, \quad (22)$$

$$[\text{O}^-] = (K_5 K_6 K_3 / K_2')[V_A^-], \quad (23)$$

$$[\text{O}^- - \text{Al}^{3+}] = [V_A^-] \left(1 + \frac{K_5 K_6 K_3}{K_2'} \right) - \frac{K_2'}{K_3} \frac{1}{[V_A^-]} + \frac{2K_3^2}{K_2'} [V_A^-]^2, \quad (24)$$

$$[\text{O} - \text{Al}^{3+}] = \frac{K_3 K_5}{K_2'} [V_A^-] \left\{ [V_A^-] \left(1 + \frac{K_5 K_6 K_3}{K_2'} \right) - \frac{K_2'}{K_3} \frac{1}{[V_A^-]} + \frac{2K_3^2}{K_2'} [V_A^-]^2 \right\}, \quad (25)$$

$$[V_A^{--}] = K_2' / K_3 K_4, \quad (26)$$

$$[V_A^-]^4 \left\{ \frac{2K_3^3 K_5}{K_2'^2} \right\} + [V_A^-]^3 \left\{ \frac{2K_3^2}{K_2'} + \frac{K_3 K_5}{K_2'} \left(1 + \frac{K_5 K_6 K_3}{K_2'} \right) \right\} + [V_A^-]^2 \left\{ 1 + \frac{K_5 K_6 K_3}{K_2'} \right\} - \{ K_5 + [\text{Al}^{3+}] \} [V_A^-] - \frac{K_2'}{K_3} = 0. \quad (27)$$

²¹ M. D. Earle, Phys. Rev. **61**, 56 (1942).

²² Hauffe *et al.*, Z. Elektrochem. **56**, 937 (1952).

TABLE II. Pressure dependence of $[V_A^-]$, $[Ti^{3+}]$, and $[O^-]$ at 1170°K; Al-doped rutile, anion vacancy model.

	Pressures in mm Hg				
	10^{-4}	10^{-3}	10^{-2}	1	10^3
$[V_A^-]$ cm $^{-3}$	1.4×10^{21}	6.8×10^{20}	3.4×10^{20}	8.5×10^{19}	9.0×10^{18}
$\frac{K_2'}{K_3} \frac{1}{[V_A^-]}$: $[Ti^{3+}]$ cm $^{-3}$	2.1×10^{21}	1.4×10^{21}	8.8×10^{20}	3.5×10^{20}	1.1×10^{20}
$\frac{K_5 K_6 K_3}{K_2'}$ $[V_A^-]$: $[O^-]$ cm $^{-3}$	1.8×10^{13}	2.9×10^{13}	4.4×10^{13}	1.1×10^{14}	3.8×10^{14}

Equations (21) to (26) give $[Ti^{3+}]$, $[V_A^-]$, $[O^-]$, $[O^- - Al^{3+}]$, $[O - Al^{3+}]$, $[V_A^-]$ as functions of $[V_A^-]$ and the equilibrium constants K_2' , K_3 , K_5 , K_6 , K_4 . Equation (27) is an equation for $[V_A^-]$ in terms of the reaction constants and the concentration of Al in the crystal $[Al^{3+}]$. This Al concentration is presumed known. The pressure dependence of the concentration of defects comes about through the term K_2' which varies as $p^{-1/2}$. To calculate numerical values, the reaction constants must be known. These may be evaluated using simplifying assumptions and such a procedure is outlined in Appendix I. It is shown there that for a reasonable choice of reaction constants, $[Ti^{3+}] \propto p^{-0.19}$ (and consequently $[O^-] \propto p^{+0.19}$). This pressure dependence is about that observed at low and at high pressures, respectively, where "low" and "high" pressures are considered with respect to the conductivity minimum. In addition, the hole concentration is also seen to be rather small, even at the highest pressures (Table II). Experimentally, σ at $p = 10^3$ mm Hg equals $10^{-2.5} \Omega \text{ cm}^{-1}$ (Fig. 4). Assuming just hole conduction to occur at high pressures—which is not inconsistent with the thermoelectric power data (Fig. 4)—the hole mobility is given by $\mu_p = \sigma_p / pe$ where σ_p is the hole conductivity at high pressures, p is the density of holes, and e is the electronic charge. Setting $\sigma_p = 10^{-2.5}$ and $p = 1.1 \times 10^{14}$ we obtain $\mu_p = 180 \text{ cm}^2/\text{V sec}$. The electron mobility at room temperature is of the order⁶ $1 \text{ cm}^2/\text{V sec}$. This mobility will decrease with an increase in temperature somewhat like T^{-1} where T is the absolute temperature⁶ so that at 1000°K, μ_n will be some fraction of $1 \text{ cm}^2/\text{V sec}$. Thus, from this development an indication is obtained that the hole mobility is considerably larger than the electron mobility at high temperatures. Assuming the high-temperature polar scattering formula to hold (cf., Sec. IV and reference 24) and also assuming the calculated value of μ_p to be correct, it is found that m_p^* is $10^{-2} m_0$, where m_0 is the free electron mass. This is a rather small effective mass; however, one would expect the hole to have a smaller effective mass than the electron since we believe it travels in a broad $2p$ band of the oxygen ions as opposed to the electrons which move in a narrow $3d$ band of the titanium ions.

(b) Titanium Interstitials, $Al^{3+}O^-$ Acceptors

The reaction of the crystal with its surrounding oxygen atmosphere may take place according to Eq. (1) [cf., pure rutile, Case 1a] or, alternately, it may take place according to Eq. (12) for the titanium interstitials model [cf pure rutile, Case 1b]. We now consider the latter case. The set of equations governing the behavior of the defects with pressure is, then, given by Eqs. (13), (17), (18), (20), and the revised electroneutrality condition:

$$[Ti^{3+}] + [O^- - Al^{3+}] = [O^-] + 4[Ti_{int}^{4+}]. \quad (28)$$

Writing, for convenience, $K_1' = K_1(T)p^{-1}$, $[Ti^{3+}]$ and $[O^-]$ are then given (in terms of $[Al^{3+}]$ and the various reaction constants) by the following equations:

$$[O^-]^6 \frac{4K_1'}{(K_5 K_6)^4} + \frac{4K_1' K_6}{(K_5 K_6)^4} [O^-]^5 + [O^-]^3 + K_6 [O^-]^2 - [O^-] \{K_5 K_6 + [Al^{3+}] K_6\} - K_5 K_6^2 = 0, \quad (29)$$

$$[Ti^{3+}] = K_5 K_6 / [O^-]. \quad (30)$$

We will not attempt to solve this system in detail (as for the previous Al-doped anion vacancy model), since an estimate of the reaction constant for Eq. (12) is difficult. However, it is clear from an inspection of Eq. (29) that the titanium interstitials model can in principle approximate the observed pressure dependence of Al-doped rutile (e.g., by retaining only the first and fifth terms in the equation). Thus, it is possible that a complete solution using the interstitials model will give agreement with experiment for the doped crystal.

IV. GENERAL CONSIDERATIONS CONCERNING THE ELECTRICAL CONDUCTIVITY AND THE THERMOELECTRIC POWER

From the foregoing considerations, we have seen that in Al-doped rutile, $[Ti^{3+}]$ (and therefore $[O^-]$) depends on a fractional power of the pressure, negative for $[Ti^{3+}]$ and positive for $[O^-]$. This characteristic dependence has important consequences in the analysis and in our attempt to fit a two-band theory to our experimental results.

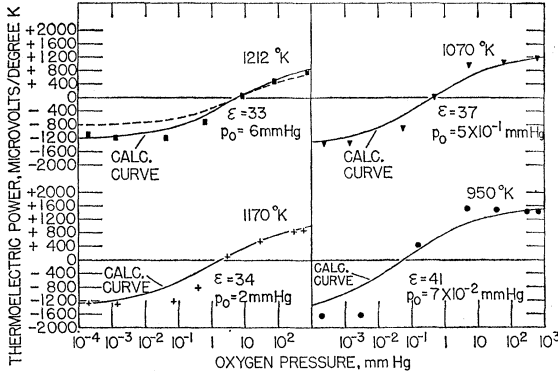


FIG. 6. Al-doped crystal, 0.5 at.%. Comparison of experimental oxygen pressure dependence of thermoelectric power Q and pressure dependence of Q calculated using the relation

$$Q = \frac{k}{2e} \left[\epsilon \frac{p^{2/5} - p_0^{2/5}}{p^{2/5} + p_0^{2/5}} - \ln \frac{p^{2/5}}{p_0^{2/5}} \right].$$

p_0 is the pressure at which $Q=0$; ϵ is determined by the energy gap, the temperature and scattering factors. ϵ is calculated using as the energy gap 3.0 eV and assuming $A_n = A_p = 2$ (p_0 and ϵ are given for each of the four temperatures at which measurements were made). The dashed curve at 1212°K represents the calculated Q values when $E_G = 2.4$ eV.

Becker and Frederikse²³ have shown that, if one uses a 2-band model and considers the dependence of the thermoelectric power Q and electrical conductivity σ on the ratio of hole to electron conductivity $\sigma_p/\sigma_n \equiv \alpha$, then expressions for Q and σ can be obtained which do not depend on the particular model of defects that is chosen. These are

$$Q = \frac{k}{2e} \left(\frac{\alpha - 1}{\alpha + 1} \right) + \delta - \ln \alpha, \quad (31)$$

$$\epsilon = (E_G/kT) + A_n + A_p,$$

$$\delta = A_p - A_n + \ln(N_V/N_C b),$$

where E_G is the intrinsic gap; A_n , A_p are scattering factors; N_V , density of states in valence band; N_C , density of states in conduction band; b , mobility ratio: μ_n/μ_p ; k is Boltzmann's constant; e is the electron charge.

$$\sigma = \sigma_i [b^{1/2}/(b+1)] [(\alpha+1)/\alpha^{1/2}], \quad (32)$$

where σ_i is the intrinsic conductivity. For the case where the density of electrons depends on the oxygen pressure p according to the form $p^{-1/x}$ (and, therefore, the density of holes goes as p^{1+x}), where x is a number that depends on the defect mechanism giving rise to the charge carriers, these authors show that α is related to the equilibrium oxygen pressure p by

$$\alpha = p^{2/x} / p_0^{2/x_0},$$

where the subscript 0 refers to the values at the mini-

mum in conductivity. In terms of oxygen pressure, then, Q and σ are given by

$$Q = \frac{k}{2e} \left(A \frac{p^{2/x} - p_0^{2/x_0}}{p^{2/x} + p_0^{2/x_0}} \right) - 2x^{-1} \ln p + 2x_0^{-1} \ln p_0, \quad (33)$$

$$\sigma = B \left(\frac{p^{1/x}}{p_0^{1/x_0}} + \frac{p^{-1/x}}{p_0^{-1/x_0}} \right). \quad (34)$$

A and B are constants which depend on band parameters, x depends on the defect mechanism assumed in the formation of the charge carriers while x_0 and p_0 are the values of x and p at the conductivity minimum. A fit to the data has been attempted in Figs. 6 and 7, using the expressions (33) and (34). The results are in reasonable agreement when the value of x is taken ~ 5 . The thermoelectric power Q has been calculated with an energy gap E_G of 3.0 eV. If the value of 2.4 eV is used, as seems more appropriate considering the fact that the measurements were at $\sim 1000^\circ\text{K}$ (cf., reference 25), the fit of the calculated curve to the experimental curve is not as good. (See Fig. 6.)

An insight into the scattering mechanism at these temperatures is obtained from a combination of thermoelectric power and conductivity data. The minimum in conductivity occurs when $\alpha = 1$. From Eq. (31), for this value of α , Q is given by

$$(2e/k)Q = \delta = A_p - A_n + \ln(N_V/N_C)b^{-1}.$$

Assuming $A_p \sim A_n$,

$$(2e/k)Q = \ln(N_V/N_C)b^{-1} = \ln(m_p^*/m_n^*)^{3/2}b^{-1},$$

where m_p^* is the hole's effective mass, m_n^* is the electron's effective mass. For a slow electron in a polar material and for high temperatures ($kT \gg k\theta$ where

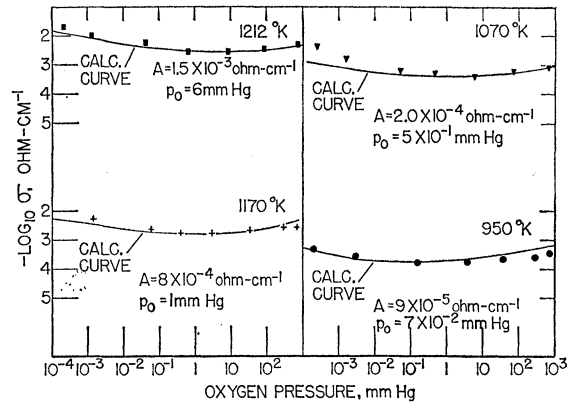


FIG. 7. Al-doped crystal, 0.5 at.%. Comparison of experimental oxygen-pressure dependence of electrical conductivity, σ , and pressure dependence of σ calculated using the relation $\sigma = A [p^{1/5}/p_0^{1/5} + p^{-1/5}/p_0^{-1/5}]$. p_0 is the pressure at which the conductivity minimum occurs and A is a constant determined by the value of σ at that point. (p_0 and A are given for each of the four temperatures at which measurements were made.)

²³ J. H. Becker and H. P. R. Frederikse, Suppl. J. Appl. Phys. 33, 447 (1962).

θ is the Debye temperature), the mean free path is given by²⁴

$$\bar{l} = \frac{3}{2} [(\epsilon \cdot \epsilon_\infty) / (\epsilon - \epsilon_\infty)] a_0; \quad kT \gg k\theta,$$

$a_0 =$ Bohr orbit $= \hbar^2 / m_e^2$, $\epsilon =$ static dielectric constant, $\epsilon_\infty =$ optical dielectric constant. The mobility of the electron is, according to this picture:

$$\mu_n = \frac{e \bar{l}}{m_n^* \sqrt{3} kT / m_n^*} = \frac{e \hbar^2 3 \epsilon \epsilon_\infty}{\sqrt{3} kT e 2 \epsilon - \epsilon_\infty} m_n^{*-3/2}.$$

If one assumes that in a similar fashion, $\mu_p \propto m_p^{*-3/2}$ where the subscript p refers to holes, then

$$b \equiv \mu_n / \mu_p = (m_p^* / m_n^*)^{3/2}.$$

For $kT \ll k\theta$ the same result obtains. Accordingly, with the assumption that $A_n \sim A_p$ at the conductivity minimum, we have for Q

$$(2e/k)Q' = \ln[(m_p^* / m_n^*)^{3/2} b^{-1}] = 0.$$

There seem to be indications that this is indeed the case (Fig. 4). However, the conductivity minimum is so broad that the determination of its exact location is difficult. Thus, it is clear that more data of both the thermoelectric power and of the conductivity in the region of the minimum is necessary before a definite statement that the thermoelectric power is zero at the conductivity minimum may be made. Becker and Frederikse²³ first considered this point and showed that if Q were zero at the conductivity minimum then $b = (m_p^* / m_n^*)^{3/2}$. They considered the polar scattering formula for the case $k\theta \gg kT$. As it has been mentioned above the results deduced obtain whether $k\theta \gg kT$ or (more appropriately for the present measurements) $kT \gg k\theta$ ($\theta \sim 600 - 700^\circ\text{K}$ ⁶ and our measurements were made at $\sim 1000^\circ\text{K}$).

V. CONCLUSIONS

Two defect models for the production of charge carriers in pure and Al-doped rutile are discussed in this paper. It is shown that in pure rutile on the basis of a given choice of reaction constants the anion vacancy model seems to predominate at pressures > 10 mm Hg while at lower pressures the titanium interstitials model is dominant. For Al-doped rutile such a distinction between the two models is not evident. There are some indications that the hole mobilities ~ 180 cm²/V sec at 1000°K . As a consequence of this, an effective mass for

the hole $\sim 10^{-2}m_0$ is deduced, assuming high-temperature polar scattering to take place. These hole mobilities are considerably larger than those expected for electrons at those temperatures. The 2-band formalism of Becker and Frederikse²³ is applied to an analysis of the data and shown to be in reasonable conformity with the observations.

ACKNOWLEDGMENTS

The author wishes to thank J. H. Becker and A. H. Kahn of the Solid State Physics Section, National Bureau of Standards, for stimulating discussions concerning this work. A careful review of the manuscript by J. H. Becker proved useful to the author and is greatly appreciated. Finally, thanks are due D. E. Roberts of the above-named section who made these experiments possible by growing the crystals studied.

APPENDIX I: DISCUSSION ON REACTION CONSTANTS USED IN CALCULATING $[\text{Ti}^{3+}]$ AND $[\text{O}^-]$, ANION VACANCY MODEL, Al-DOPED RUTILE

K_2' and K_3 are obtained exactly as in our discussion for pure nonstoichiometric rutile. K_4 is obtained in a similar way to K_3 assuming that V_A^{--} is like an un-ionized helium atom in a medium of dielectric constant 70. K_5 is obtained in a similar fashion assuming Al^{3+}O^- behaves as a hydrogen atom in a medium of dielectric constant 70. K_6 may be evaluated if one knows the intrinsic reaction constant K_i and also K_5 . From Eqs. (17) and (18), $K_5 K_6 = [\text{Ti}^{3+}][\text{O}^-]$. If one considers the intrinsic reaction, viz., $\text{Ti}^{4+} + \text{O}^{--} \rightleftharpoons \text{Ti}^{3+} + \text{O}^-$, the law of mass action gives $[\text{Ti}^{3+}][\text{O}^-] = K_i(T)$. Thus $K_5 K_6 = K_i$. K_i is given by³

$$K_i = 4 \left(\frac{2\pi kT}{\hbar^2} \right)^3 (m_p^*)^{3/2} (m_n^*)^{3/2} \exp(-E_G/kT),$$

where m_p^* and m_n^* are the hole and electron effective masses, respectively, E_G is the intrinsic energy gap and the other symbols have their usual meaning. m_n^* at ordinary temperatures $\sim 30m_0$;^{6,7} at 1000°K its value is probably somewhat different. Assume, however, a value $m_n^*(1000^\circ\text{K}) = 30m_0$. Furthermore, since the hole is thought to be traveling in the broad $2p$ band of the oxygen ions, $m_p^* \sim m_0$ and probably somewhat less; assume $m_p^* = m_0$. We still need a value of E_G if K_i is to be determined. E_G at 0°K is^{5,6} 3.0 eV and decreases with increasing temperature. According to the data in Fig. 4 of the paper by von Hippel *et al.*,²⁵ $E_G \sim 2.4$ eV at 1000°K . With these values, $K_i(1170^\circ\text{K}) = 2.44 \times 10^{32}$ cm⁻⁶. The pressure dependence of the various defects may now be calculated using the equations in the text

²⁴ H. Fröhlich *et al.*, Phil. Mag. 41, 221 (1950). These authors state that "The remarkably simple result leads to values of λ of the order 5×10^{-8} cm. This is appreciably smaller than the de Broglie wavelength of thermal electrons at room temperature. The quantitative agreement [of this relation with experiment] is, therefore, doubtful." However, if one compares \bar{l} calculated at 1000°K for an electron of effective mass $50 m_0$ with the de Broglie wavelength λ of the same heavy electron at 1000°K , the agreement between λ and \bar{l} is good.

²⁵ See reference 7. The temperature variation of the energy gap (dE/dt) was determined by plotting $\hbar\nu$ at the three optical densities 0.6, 1.0, 2.0 vs temperature. dE/dt was found to be the same to a good approximation for the three optical densities chosen and equal to 7×10^{-4} eV/deg K.

TABLE III. Estimate of reaction constants at 1170°K for Al-doped rutile, anion vacancy model.

K_2' :	$2.4 \times 10^{61} p^{-1/2}$,	$p = \text{pressure in mm Hg}$
K_3 :	$8 \times 10^{20} \text{ cm}^{-3}$	
K_4 :	$3.5 \times 10^{21} \text{ cm}^{-3}$	
K_5 :	$8 \times 10^{21} \text{ cm}^{-3}$	
K_6 :	$3.1 \times 10^{10} \text{ cm}^{-3}$	
K_i :	$2.4 \times 10^{32} \text{ cm}^{-6}$	

(Case 2. Al-doped nonstoichiometric rutile in Sec. III). The constants used in this calculation are grouped together in Table III. The results for $[V_A^-]$ and for $[Ti^{3+}]$ (electron concentration) and $[O^-]$ (hole concentration) are given in Table II. It is found that $[V_A^-] \propto p^{-1/3.2}$. Since $[Ti^{3+}] = (K_2'/K_3)[V_A^-]^{-1}$ it is seen that $[Ti^{3+}] \propto p^{-0.19}$ and that, consequently, $[O^-] \propto p^{+0.19}$.

Superconductivity in the Mercury-Indium Alloy System*

M. F. MERRIAM, M. A. JENSEN, AND B. R. COLES†
University of California, San Diego; La Jolla, California
 (Received 28 January 1963)

The superconducting transition temperatures of a large number of Hg-In alloys have been measured and the variation of T_c with composition determined over the entire range. Variation of T_c with number of valence electrons/atom within any particular metallurgical phase is quite strong, T_c in general increasing with decreasing number of valence electrons. The maximum and minimum values of T_c occurring in the system are 4.5 and 3.1°K at approximately 80 and 20 at.% indium, respectively. HgIn, the only stoichiometric compound, has a transition temperature of 3.81°K. The observed composition dependence of T_c is not what one would expect either from Matthias's empirical rules or from the simple BCS formula, assuming a nearly free electron model for the density of states. In one phase a discontinuity in T_c and its composition dependence is found which cannot be correlated with a change in any lattice property and apparently arises from a discontinuous change in electronic structure. In connection with the problem of the effect of one phase upon superconductivity in another with which it is in intimate contact, there is evidence that the transition temperature of HgIn can be lowered a few tenths of a degree if large quantities of a lower transition temperature phase are also present. Electrical conductivity data, which were obtained in the course of the superconductivity measurements by an induced-current method, made possible also the determination of residual resistivity over the entire composition range.

INTRODUCTION

SEVERAL detailed studies of the variation of superconducting transition temperature, T_c , with composition in binary transition metal alloy systems^{1,2} have been made in recent years. Although the dependence of T_c on composition cannot yet be deduced in an unambiguous way from first principles, or even from the BCS model,³ a certain degree of empirical understanding has been achieved. In particular, the rule of Matthias,⁴ connecting T_c with average number of valence electrons per atom, has been remarkably successful in predicting transition temperature variation in a large number of binary and ternary transition metal alloy systems. Experimental work has been concentrated on alloys and intermetallic compounds with at

least one transition metal component, primarily because of the extensive ranges of solid solubility and the sets of isostructural compounds which are associated with transition metals and which are much less common in alloy systems of the nontransition metals. The alloying behavior of the transition elements facilitates comparison of different superconductors since variations in crystal structure can readily be avoided.

Even in binary transition metal systems where several different phases occur, for example Mo-Re, the superconducting transition temperature is found to vary predominately according to the variation of n (average number of valence electrons per atom) following Matthias' rule.⁴ Discontinuous changes in T_c occur at changes of phase but these are usually small compared with the over-all variation.

Data already available indicated that the dependence of T_c on n is less pronounced in alloy systems of the nontransition metals, than in alloy systems with a transition metal component. No comprehensive study had, however, been made over the entire composition range of a nontransition-metal alloy system, and so we decided to investigate the mercury-indium system.

In order to interpret the transition temperature

* Research supported in part by the U. S. Air Force Office of Scientific Research and the National Science Foundation.

† Permanent address: Physics Department, Imperial College, London, England.

¹ J. K. Hulm and R. D. Blaugher, *Phys. Rev.* **123**, 1569 (1961).

² G. F. Hardy and J. K. Hulm, *Phys. Rev.* **93**, 1004 (1954).

³ J. Bardeen, L. N. Cooper, and J. R. Schrieffer, *Phys. Rev.* **106**, 162 (1957); **108**, 1175 (1957).

⁴ B. T. Matthias, in *Progress in Low Temperature Physics*, edited by C. J. Gorter (North-Holland Publishing Company, Amsterdam, 1957), Vol. 2.